

# Temperature dependent charge transport in organic field-effect transistors with the variation of both carrier concentration and electric field

Mamatimin Abbas<sup>1,2</sup>, Almantas Pivrikas<sup>1,3</sup>, Elif Arici<sup>1,6</sup>, Nalan Tekin<sup>4</sup>,  
Mujeeb Ullah<sup>5</sup>, Helmut Sitter<sup>5</sup> and Niyazi Serdar Sariciftci<sup>1</sup>

<sup>1</sup> Linz Institute for Organic Solar cells, Johannes Kepler University Linz, Altenbergerstr. 69, Linz 4040 Austria

<sup>2</sup> Laboratoire IMS, Université Bordeaux 1, UMR 5218 CNRS, ENSCBP, 16 Avenue Pey-Berland, 33607 Pessac Cedex, France

<sup>3</sup> School of Chemistry and Molecular Biosciences, Centre For Organic Photonics and Electronics (COPE), The University of Queensland, Brisbane 4072, Australia

<sup>4</sup> Department of Chemistry, Faculty of Arts and Sciences, Kocaeli University, 41380 Kocaeli, Turkey

<sup>5</sup> Institute of Semiconductor Physics, Johannes Kepler University Linz, Altenberger str. 69, Linz 4040 Austria

<sup>6</sup> Energy Institute, Istanbul Technical University, Ayazaga Kampüsü, 34469 Maslak, Istanbul, Turkey

E-mail: [mamatimin.abbas@ims-bordeaux.fr](mailto:mamatimin.abbas@ims-bordeaux.fr)

Received 6 September 2013, in final form 30 September 2013

Published 15 November 2013

Online at [stacks.iop.org/JPhysD/46/495105](http://stacks.iop.org/JPhysD/46/495105)

## Abstract

We present experimental evidence of combined effects of temperature, carrier concentration, electric field as well as disorder on charge transport in an organic field-effect transistor (OFET). Transfer characteristics of an OFET based on sexithiophene active layer were measured from 80 to 300 K. Thermally activated carrier mobility followed Arrhenius law with two activation energies. Carrier density variation led to finite extrapolated Meyer–Neldel (MN) temperature (780 K) at low fields. Negative electric field-dependent mobility was observed in available field range. MN temperature shifted towards higher temperature when the electric field increased, and did not retain its finite character above the field of  $4 \times 10^3 \text{ V cm}^{-1}$ .

(Some figures may appear in colour only in the online journal)

## 1. Introduction

Understanding the charge transport mechanism in amorphous organic semiconductors is not only essential in formulating fundamental scientific concepts, but also in tailoring the properties to improve the performance of the opto-electronics devices based on these materials. Mobility is the focal parameter in charge transport. Its dependence separately on temperature, carrier concentration and electric field has been studied extensively [1–3]. When both temperature and carrier concentration come into the picture, charge transport behaviour is reflected by the presence of Meyer–Neldel (MN) compensation rule [4–6, 8]. Organic field-effect

transistors (OFETs) allow one to finely tune the charge carrier concentration by gate voltage variation, while drain voltage controls the electric field. Moreover, OFETs are the main components of organic electronic devices, where the charge carrier mobility is directly relevant for their performance. MN temperature has been reported in OFET devices, which operate in the range of high carrier concentration and weak electric field [5, 6]. Such a phenomenon has been elucidated by both generalized adiabatic polaron hopping [7] and disorder model with effective medium approximation [8]. It is even directly correlated to the disorder parameter in the latter model, which used zero field approximation. Experimental evidence supports such a model [9]. Carrier density and

electric field effects should be incorporated in order to provide a complete picture of charge transport mechanism in this system. Recent investigations on a fullerene field-effect transistor, where the active layer has high mobility polycrystalline nature (mobility around  $1 \text{ cm}^2 \text{ V}^{-1} \text{ s}^{-1}$ ), show Poole–Frenkel-type dependence on the electric field [12], leading to the decrease of the MN temperature with the increase of the electric field [11]. An analytical model considering spatial energy correlation addressed such a collective effect given that Poole–Frenkel-type dependance is obeyed in OFET structure [10]. Using a more disordered active layer (mobility around  $10^{-3} \text{ cm}^2 \text{ V}^{-1} \text{ s}^{-1}$ ), in this work, we present a rather different behaviour of charge carrier mobility dependance on temperature, carrier concentration and electric field, where the MN temperature shifts towards infinity when the electric field is increased.

## 2. Experimental

Sexithiophene (6T) was purchased from Sigma-Aldrich, purified through vacuum tube sublimation, followed by further purification in high vacuum system (see figure 1(a) for chemical structure). We used poly(1-vinyl-1,2,4-triazole) (PVT) as dielectric layer (see figure 1(b) for chemical structure). PVT has low leakage current, high breakdown voltage. OFET devices based on PVT are lacking hysteresis with very low threshold voltages for both n- and p-channel devices [13, 14]. Bottom gate, top contact OFET device structure is shown in figure 1(c). Al gate contact (100 nm thick) was vacuum evaporated on pre-cleaned glass substrate through a shadow mask (1 mm wide and 13 mm long). PVT ( $70 \text{ mg ml}^{-1}$  in pure water) was spin coated at 1500 rpm for 60 s. The film was dried in a low-vacuum oven overnight at  $50^\circ\text{C}$ . 80 nm thick 6T film was evaporated on PVT surface with  $0.5 \text{ \AA s}^{-1}$  evaporation rate at room substrate temperature in a Univex system at a base pressure of  $2 \times 10^{-6}$  mbar. Au (100 nm) as sources/drain contacts were evaporated thermally through shadow mask to complete the device. Channel length is 0.05 mm and channel width is 3 mm.  $I$ – $V$  characterizations were performed using Agilent E5273A system in glove box prior to mounting it in a cryostat (Oxford).

## 3. Results and discussions

Transfer and output characteristics were measured at every 10 K step, allowing about an hour in between for the stabilization of the device temperature. Stability of the device during the temperature variation is shown in figure 2. After the first cycle (300 K–80 K–300 K), we observed decrease in the off current, probably due to volatile dopants. The transfer curve is almost the same after the second cycle, showing the stability of the device, and the data presented are from this cycle of measurements.

Gate voltage dependant carrier mobility can be determined by gradual channel approximation given as the formula below:

$$\mu_{\text{lin}} = \frac{L}{C_i W V_{\text{ds}}} \frac{\partial I_{\text{ds}}}{\partial V_{\text{gs}}},$$

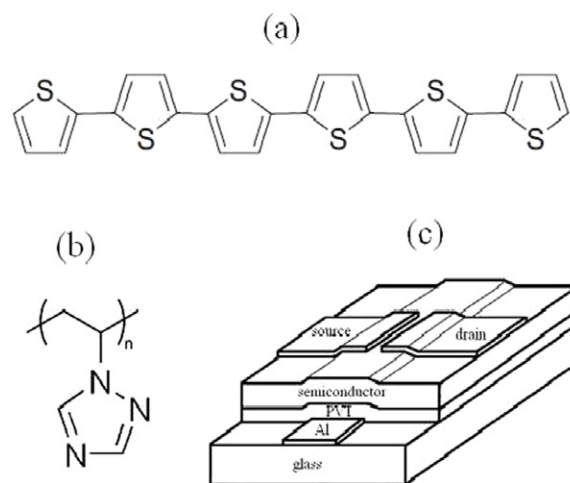


**Figure 1.** (a) Chemical structure of  $\alpha$ -sexithiophene (6T); (b) poly(1-vinyl-1,2,4-triazole)(PVT); (c) bottom gate, top contact OFET device structure used in this work.

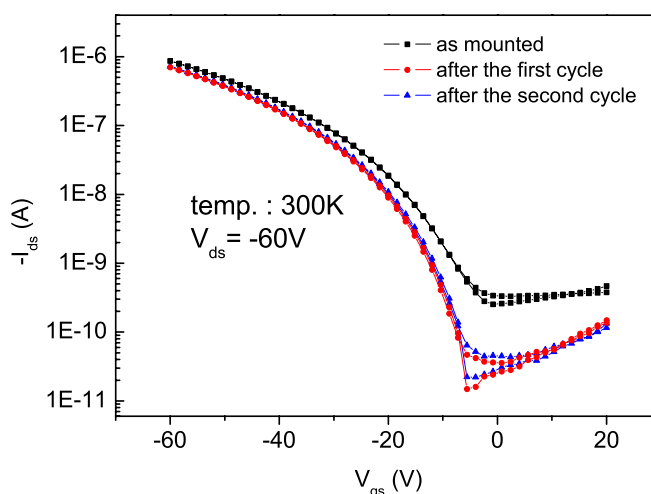


**Figure 2.** Transfer characteristics of the OFET device in saturation regime at 300 K after mounting it in a cryostat, the first cycle (300 K–80 K–300 K) and the second cycle of measurements.

where  $I_{\text{ds}}$  is the drain current;  $W$  is the channel width (3 mm);  $L$  is the channel length (0.05 mm);  $\mu(V_{\text{gs}})$  is the gate voltage dependent mobility;  $C_i$  is the dielectric capacitance in unit area ( $5 \text{ nF cm}^{-2}$ );  $V_{\text{gs}}$  is the gate voltage.

We present in figure 3 the gate voltage dependent mobility of the device for 300 K, 190 K and 80 K, respectively in linear regime at  $V_{\text{ds}} = -10 \text{ V}$ . We did not observe saturation behaviour at higher gate voltage which is common for most of the reported OFET devices due to contact resistance. Moreover, the quasi linear increase of the mobility is similar to the characteristics of the devices where simulation was carried out to remove the effect of the contact resistance in the previous reports [16, 17]. Contact resistance is an important factor to be taken into account for the mobility estimation of the OFET devices, higher value of which leads to underestimation of the mobility at high gate voltages. Staggering configuration is indeed reported to give much smaller contact resistance comparing to the co-planer configuration [15]. That is

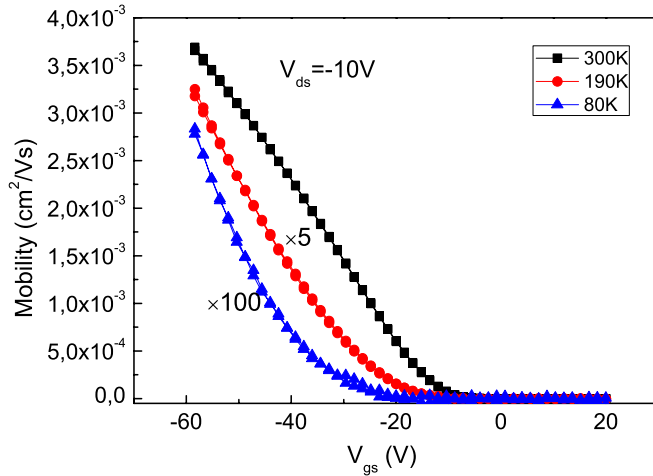


**Figure 3.** Gate voltage dependent mobility of 6T at 300 K, 190 K and 80 K, respectively in linear regime at  $V_{ds} = 10$  V.

the reason we used staggering (bottom gate, top contact) configuration for our device. We annealed the device at 100 °C for ten minutes in inert condition to further decrease the effect. Moreover, very smooth surface of PVT dielectric with root-mean-square roughness of about 0.2 nm guarantees minimum contact resistance induced by surface roughness [13]. The difference in the slope for the different temperatures, which is due to the temperature dependance of the mobility variation in terms of carrier concentration, is a subject for later discussions.

Figure 4 shows the output characteristics of the device both at room (300 K, left panel) and low temperatures (80 K, right panel) with well defined saturation, a further proof for our device quality.

In figure 5(left panel), we show the transfer characteristics of the device at various temperatures from 80 to 300 K at  $-10$  V source–drain voltage. The on/off ratio of the device at room temperature is more than  $10^5$ , and rather appreciable at lower temperatures. Source–drain voltage (field along the channel) is varied from  $-5$  to  $-20$  V, and transfer characteristics for the case at 300 K is shown in figure 5(right panel). We argue that increasing the field along the channel does change the charge carrier distribution within the channel. However, charge carriers are concentrated just in a few layers at the interface of the semiconductor and the dielectric; therefore, increasing the field rather before the pinch-off of the channel has a very minor effect on the charge carrier distribution profile within the channel, so as to introduce diffusion effect for static transport in an OFET device.

Temperature dependant mobilities at various gate voltages (carrier concentrations) are presented in figure 6(left panel). Arrhenius behaviour is observed with two distinct activation energies at the transition temperature of about 190 K. This transition temperature is also observed in previous study [18], which can be correlated to a phase transition. Gate voltage dependant activation energies (around 100 and 70 meV) of these two phases are shown in the inset of figure 6(left panel). Below 100 K, the transport seems to deviate from purely thermal activation, an indication from hopping to

tunnelling crossover. By varying the carrier concentration with different gate voltages, we obtained a common so-called MN temperature where the mobility is independent of carrier concentration. Figure 6(right panel) shows the temperature dependance of the mobility with respect to the variation of the electric field with convergence of the mobility at a finite temperature at high carrier concentration. It has to be noted that the mobility decreases with the increase of the electric field within the available electric field range. Charge carriers can find percolation pathways when they encounter structural defects. Such pathways are limited when electric field enforces directionality for the charge carrier transport. Therefore, at higher electric fields, more charge carriers can be trapped at the defect sites, leading to the decrease in the mobility. Higher degree of spatial disorder enhances the effect [19]. Negative field dependence of mobility was also observed in polymer diode device [20].

First activation energy region above the transition temperature of 200 K is used to derive the MN temperature. Gate voltage range has been extended further down to  $-28$  V as the threshold voltages fall below this value within considered temperature range. Figures 7(a), (b), (c) and (d), respectively shows the MN temperature dependence on the electric field. Obviously it is a rather sensitive parameter with respect to the electric field, which does not retain its finite character when the field is increased to about  $4 \times 10^3$  V cm $^{-1}$ , a phenomenon not observed before. Threshold voltage, which mainly accounts for the total trap densities, increases following the decrease of the temperature, therefore, another important consideration can be replacing gate voltage variation with effective gate voltage, i.e.  $V_{gs} - V_{th}$ , in order to exclude the amount of carriers used for filling the traps. Here, threshold voltages were derived from saturation transfer curves, and difference in each temperature was taken into account. Such a treatment resulted in no finite MN temperature, even at low electric field (as shown in the inset of figure 7(a)), indicating that MN temperature originates from the trap states in amorphous semiconductors. Here we would like to stress that MN temperature is not a physical parameter, rather an apparent one. However, as a very sensitive value for electric field variation, it is an essential parameter for theoretical description of charge transport in a disordered system. At  $-5$  V of drain–source voltage, MN temperature is about 780 K, which is rather high compared to the work on the fullerene field-effect transistor, where it has a typical value of about 400 K [9]. Such a discrepancy arises mainly due to the very different structural order of the active layers in these studies. The mobility of charge carriers is about three orders of magnitude lower in this work, reflecting a more disordered system. Indeed, structural disorder was correlated to MN temperature in this early study where MN temperature was reported to be as low as 250 K for a highly ordered active layer [9]. However, a further study shows that when electric field increases, MN temperature decreases, contrary to our finding [11]. MN temperature reflects how the activation energies vary with the carrier concentration. Large change in activation energies gives low MN temperature. Even larger change in activation energies can be expected when the increased field constructively contributes to the

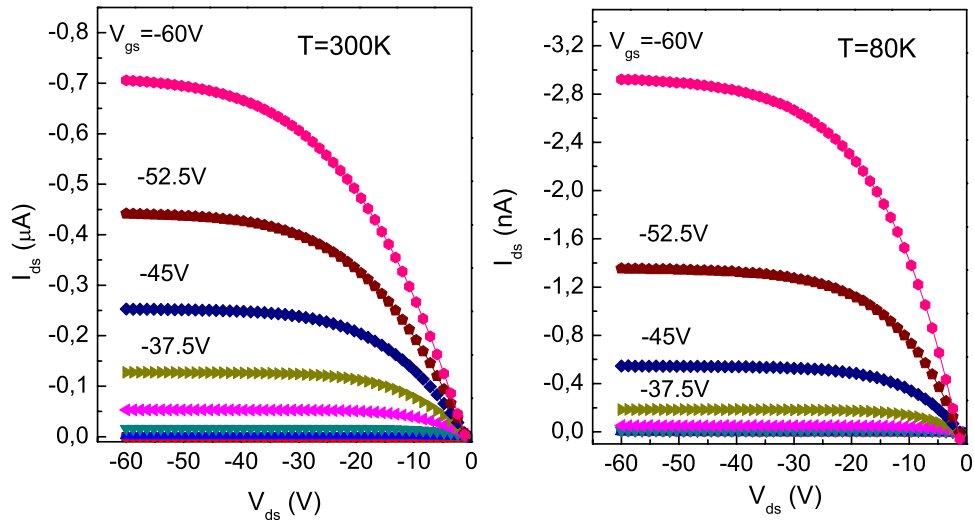


Figure 4. Output characteristics of the OFET device at 300 K (left panel) and at 80 K (right panel).

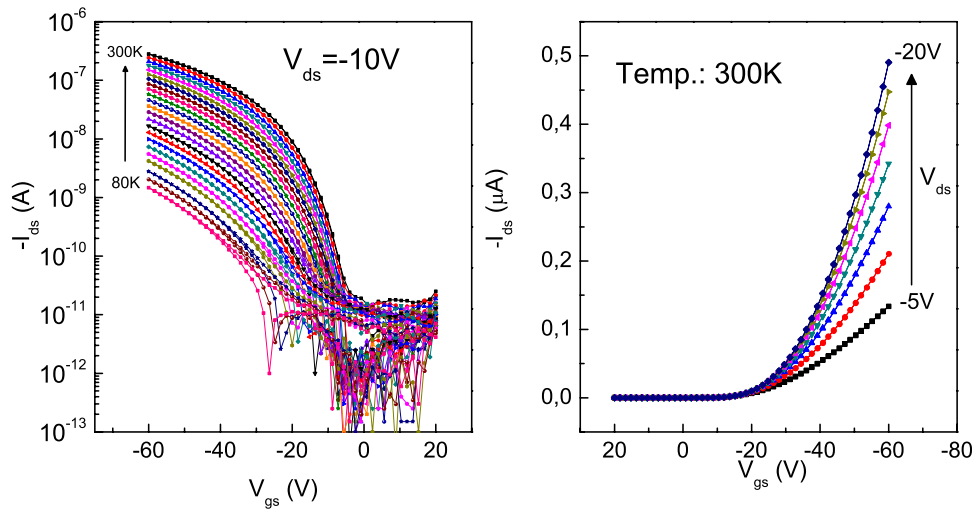


Figure 5. (left panel) Transfer characteristics (forward and backward scan) of 6 T OFET from 80 to 300 K at every 10 K step; (right panel) transfer characteristics of the device at 300 K varying applied drain-source voltage.

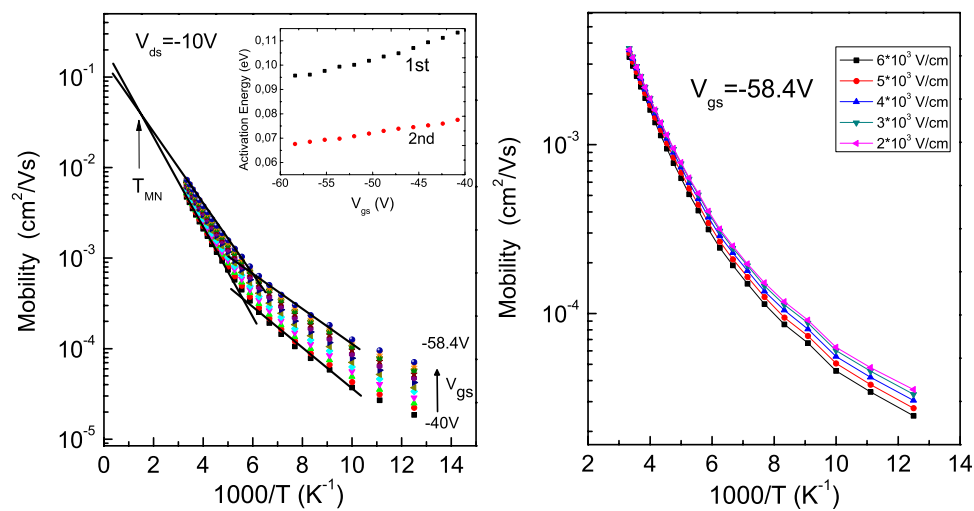
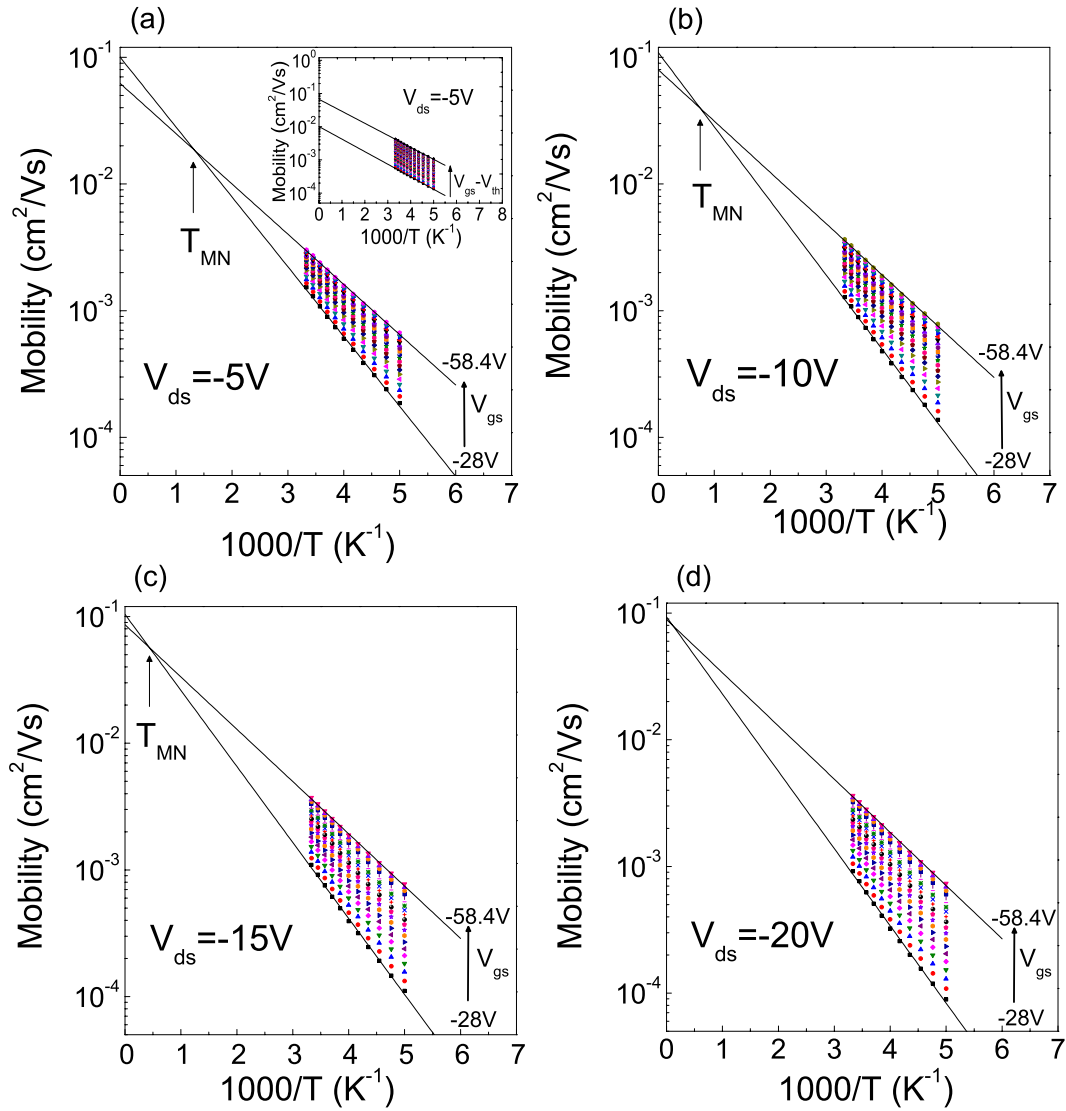


Figure 6. (left panel) Mobility versus temperature at constant drain voltage with different gate voltages (carrier concentration). Inset shows the activation energies in two phases; (right panel) mobility versus temperature at constant gate voltage with different applied drain-source voltages (electric field).



**Figure 7.** Mobility versus temperature with different gate voltages (carrier concentration) at various drain–source voltages (electric field) as indicated in respective figures. Inset of (a) shows the replacement of gate voltage variation with effective gate voltage ( $V_{gs} - V_{th}$ ) variation.

charge transport, as in the case of a highly ordered system where Poole–Frenkel–type field dependence of the mobility can be obeyed. However, in a less ordered system, as in our case, increase of the field hinders charge transport due to the directionality it enforces on the carriers, thus minimizing their percolation paths. Consequently, variation of activation energies becomes less significant when the electric field increases, leading to the increase in the MN temperature. We can conclude that there are two regimes defined by the degree of disorder, where MN temperature dependence on the electric field follows different rules. In a highly ordered system, MN temperature decreases with the increase of the electric field, given that Poole–Frenkel–type field dependence of the mobility can be obeyed, as explained by the theoretical model [10]. On the other hand, in a less ordered system where the spatial disorder dominates, MN temperature increases with the increase of the field and finally loses its finite character, yet to be addressed by a suitable theoretical model.

#### 4. Conclusions

In conclusion, we present experimental evidence of MN temperature dependence on the electric field, which incorporates temperature, carrier concentration and electric field effects on charge transport in disordered organic semiconductor. OFET devices enabled us to study the collective effects in high carrier concentration and low electric field regime. MN temperature is found to increase with the increase of the electric field, eventually losing its finite character above the field of  $4 \times 10^3$  V cm<sup>-1</sup>, which is the direct result of the mobility decrease following the increase of the electric field within the available field range. We propose that such a behaviour arises from the fact that the spatial disorder dominates in our system and a suitable theoretical model for charge transport in disordered organic semiconductor is necessary to address this phenomenon with the consideration of temperature, carrier concentration, electric field as well as degree of disorder in high carrier concentration and low electric field regime.

## Acknowledgments

The work is financially supported by Austrian Science Funds (FWF) project No P20724-N20. We are thankful for Professor A K Kadashchuk for helpful scientific discussions.

## References

- [1] Coropceanu V, Cornil J, da Silva Filho D A, Olivier Y, Silbey R and Bredas J 2007 *Chem. Rev.* **107** 926
- [2] Bäessler H 1993 *Phys. Status Solidi b* **175** 15
- [3] Bouhassoune M, van Mensfoort S L M, Bobbert P A and Coehoorn R 2009 *Org. Electron.* **10** 437
- [4] Meyer W and Neldel H 1937 *Z. Tech. Phys. (Lpz.)* **18** 588
- [5] Meijer E J, Matters M, Herwig P T, de Leeuw D M and Klapwijk T M 2000 *Appl. Phys. Lett.* **76** 3433
- [6] Ullah M, Singh T B, Sitter H and Sariciftci N S 2009 *Appl. Phys. A* **97** 521
- [7] Emin D 2008 *Phys. Rev. Lett.* **100** 166602
- [8] Fishchuk I I, Kadachchuk A, Genoe J, Ullah M, Sitter H, Singh T B, Sariciftci N S and Bäessler H 2010 *Phys. Rev. B* **81** 045202
- [9] Ullah M, Fishchuk I I, Kadashchuk A K, Stadler P, Pivrikas A, Simbrunner C, Poroshin V N, Sariciftci N S and Sitter H 2010 *Appl. Phys. Lett.* **96** 213306
- [10] Fishchuk I I, Kadashchuk A, Ullah M, Sitter H, Sariciftci N S and Bäessler H 2012 *Phys. Rev. B* **86** 045207
- [11] Ullah M, Pivrikas A, Fishchuk I I, Kadashchuk A, Stadler P, Simbrunner C, Sariciftci N S and Sitter H 2011 *Appl. Phys. Lett.* **98** 223301
- [12] Pivrikas A, Ullah M, Sitter H and Sariciftci N S 2011 *Appl. Phys. Lett.* **98** 092114
- [13] Abbas M, Cakmak G, Tekin N, Kara A, Guney H Y, Arici E and Sariciftci N S 2011 *Org. Electron.* **12** 497
- [14] Abbas M and Tekin N 2012 *Appl. Phys. Lett.* **101** 073302
- [15] Street R A and Salleo A 2002 *Appl. Phys. Lett.* **81** 2887
- [16] Horowitz G, Hajlaoui R, Fichou D and El Kassmi A 1999 *J. Appl. Phys.* **85** 3202
- [17] Mansouria S, Horowitz G and Bourguiga R 2010 *Synth. Met.* **160** 1787
- [18] Stallinga P, Gomes H L, Biscarini F, Murgia M and de Leeuw D M 2004 *J. Appl. Phys.* **96** 5277
- [19] Pautmeier L, Richert R and Bäessler H 1990 *Synth. Met.* **37** 271
- [20] Mozer A J, Sariciftci N S, Pivrikas A, Österbacka R, Juska G, Brassat L and Bäessler H 2005 *Phys. Rev. B* **71** 035214